Vol 18 No 3, March 2009
1674-1056/2009/18(03)/0975-09
Chinese Physics B
© 2009 Chin. Phys. Soc.
and IOP Publishing Ltd

A new car-following model with consideration of the traffic interruption probability*

Tang Tie-Qiao(唐铁桥)[a)b)], Huang Hai-Jun(黄海军)[b)†],
Wong S. C.(黄仕进)[c)], and Jiang Rui(姜 锐)[d)]

[a)] *School of Transportation Science and Engineering, Beijing University of Aeronautics and Astronautics, Beijing* 100083, *China*
[b)] *School of Economics and Management, Beijing University of Aeronautics and Astronautics, Beijing* 100083, *China*
[c)] *Department of Civil Engineering, University of Hong Kong, Pokfulam Road, Hong Kong SAR, China*
[d)] *School of Engineering Science, University of Science and Technology of China, Hefei* 230026, *China*

(Received 24 July 2008; revised manuscript received 20 September 2008)

In this paper, we present a new car-following model by taking into account the effects of the traffic interruption probability on the car-following behaviour of the following vehicle. The stability condition of the model is obtained by using the linear stability theory. The modified Korteweg–de Vries (KdV) equation is constructed and solved, and three types of traffic flows in the headway sensitivity space—stable, metastable, and unstable—are classified. Both the analytical and simulation results show that the traffic interruption probability indeed has an influence on driving behaviour, and the consideration of traffic interruption probability in the car-following model could stabilize traffic flow.

Keywords: car-following model, traffic interruption probability, stability
PACC: 0550, 0520

1. Introduction

So far, complex traffic phenomena have been analysed by various models and some important results have been obtained.[1] Among these models, the cellular automaton models and the car-following models are often adopted to capture the basic characteristics of vehicle motion. In the car-following models, velocity, headway, and relative velocity are the main variables and used to determine the vehicles' accelerations.[2−14] In recent years, researchers further consider other factors in the car-following models for enhancing their abilities of describing real traffic.[15−21] In addition, Han *et al* [22] presented a modified CM (coupled map) car-following model and found that their model can improve the stability of traffic flow. However, various traffic interruption factors are not considered yet. The existing models do not involve the effects of traffic interruption probability on traffic flow, so they cannot directly be used to study the complex traffic phenomena resulting from various traffic interruptions (e.g., accident, pedestrian, tolling station, signal light). In fact, some traffic interruptions always occur with some probabilities and produce complex phenomena. Wong *et al* [23−25] studied the contributing factors to traffic accidents. Telesca and Lovallo[26] analysed the temporal properties in traffic accident time series and found that the time dynamics of traffic accidents is not Poissonian but long-range correlated with periodicities ranging from 12 hours to one year. Recently, Baykal-Gürsoy *et al* [27] used the queuing theory to model traffic flow interrupted by incidents. The models proposed in Refs.[23–27] can reproduce some traffic phenomena resulting from accidents, but cannot be used to evaluate the effect of various traffic interruption factors on the car-following behaviour, since the traffic interruption probability is not considered explicitly.

In this paper, we present a new car-following model by taking into account the effects of the traffic interruption probability on the car-following behaviour of the following vehicle. By using the linear stability theory and nonlinear analyses, we obtain the neutral stability curve and the coexisting curve of the model. These curves divide traffic flow into stable, metastable, and unstable regions. Both the analytical

*Project supported by the National Natural Science Foundation of China (Grant Nos 70701002 and 70521001), the National Basic Research Program of China (Grant No 2006CB705503), and the Research Grants Council of the Hong Kong Special Administrative Region of China (Grant No HKU7187/05E).
†E-mail: haijunhuang@buaa.edu.cn

and numerical results show that the consideration of traffic interruption probability can improve the stability of traffic flow.

2. Model

In general, the single-lane car-following model can be written as follows:[1]

$$\frac{\mathrm{d}^2 x_n}{\mathrm{d}t^2} = f\left(v_n, \Delta x_n, \Delta v_n\right), \tag{1}$$

where $f(\cdot)$ is the stimulus function, x_n and v_n the position and velocity of vehicle n respectively, $\Delta x_n = x_{n+1} - x_n$ the headway, and $\Delta v_n = v_{n+1} - v_n$ the relative velocity (see Fig.1).

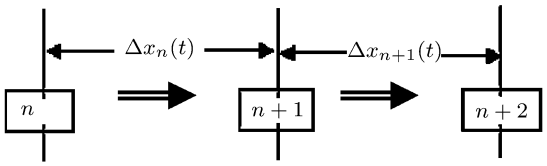


Fig.1. Schematic of the car-following model.

Note that in Eq.(1), the acceleration of a vehicle is completely determined by velocity v_n, headway Δx_n, and relative velocity Δv_n. Recently, the models with consideration of the vehicles' multiple headways have been developed as follows:[15−19]

$$\frac{\mathrm{d}^2 x_n}{\mathrm{d}t^2} = f\left(v_n, \Delta x_n, \Delta x_{n+1}, \ldots, \Delta x_{n+m}, \Delta v_n\right), \tag{2}$$

where $\Delta x_{n+i} = x_{n+i+1} - x_{n+i}$. Zhao and Gao[20] found that a collision will occur under certain given conditions when the above model is used to describe traffic flow. They then presented a modified model by considering the effect of the leading vehicle's acceleration on the following vehicle. It follows that

$$\frac{\mathrm{d}^2 x_n}{\mathrm{d}t^2} = f\left(v_n, \Delta x_n, \Delta v_n, \mathrm{d}^2 x_{n+1}/\mathrm{d}t^2\right). \tag{3}$$

For further improving the stability of traffic flow, Wang *et al* [21] proposed a multiple velocity difference model. It follows,

$$\frac{\mathrm{d}^2 x_n}{\mathrm{d}t^2} = f\left(v_n, \Delta x_n, \Delta v_n, \Delta v_{n+1}, \ldots, \Delta v_{n+k}\right), \tag{4}$$

where $\Delta v_{n+i} = v_{n+i+1} - v_{n+i}$. Numerical results have shown that the models (2)–(4) can indeed improve the stability of traffic flow in comparison with the model (1). In addition, Ge *et al* [19] declared that drivers do not necessarily consider the effects of an arbitrary number of vehicles ahead of them, but they do consider those of the three that are ahead of them.

The above car-following models can describe various complex phenomena, but cannot directly be used to study the phenomena resulting from some traffic interruption factors (e.g., accident, pedestrian, tolling station, signal light, etc.). In fact, each vehicle may be interrupted with some probability. Considering this, we rewrite the acceleration equation of the nth vehicle as follows:

$$\begin{aligned}\frac{\mathrm{d}v_n(t)}{\mathrm{d}t} =& \alpha\left[V\left(\Delta x_n\right) - v_n\right] + \lambda_1 p_{n+1}\left(-v_n\right) \\ &+ \lambda_2\left(1 - p_{n+1}\right)\Delta v_n,\end{aligned} \tag{5}$$

where p_{n+1} is the probability that the leading vehicle is interrupted, α, λ_1, λ_2 are the reactive coefficients. Once the leading vehicle is completely interrupted, its speed immediately becomes zero, i.e., the speed difference between the $(n+1)$th and the nth vehicles takes $(-v_n)$. Equation (5) states that the acceleration of the nth vehicle is determined by the speed v_n, the headway Δx_n, the relative speed Δv_n and the probability p_{n+1}. $V\left(\Delta x_n\left(t\right)\right)$ is the optimal velocity of vehicle n at time t and can be defined as follows:[2,3]

$$V(\Delta x_n) = \frac{v_{\max}}{2}\left(\tanh\left(\Delta x_n - h_{\mathrm{c}}\right) + \tanh(h_{\mathrm{c}})\right), \tag{6}$$

where h_{c} is the safe distance of headway and $v_{\max}$ is the maximum speed. Note that this headway-induced optimal velocity has the following properties:

(i) it is a monotonically increasing function of headway Δx_n and bounded by the maximal velocity $v_{\max}$;

(ii) it has a turning point at $\Delta x_n = h_{\mathrm{c}}$, i.e.,

$$V''(h_{\mathrm{c}}) = \left.\frac{\mathrm{d}^2 V(\Delta x_n)}{\mathrm{d}\Delta x_n^2}\right|_{\Delta x_n = h_c} = 0. \tag{7}$$

As explained in Ref.[19], the reason to choose Eq.(6) is that it has a turning point at $\Delta x_n = h_{\mathrm{c}}$, which is important for deriving the Burgers, KdV, and mKdV equations from Eq.(5).

The traffic interruption probability is related to traffic condition and road configuration. For simplicity, we assume in this paper that the traffic interruption probability is a constant, i.e., $p_{n+1} = p_0$. For conducting stability analysis of Eq.(5), we discretize it using the asymmetric forward difference. It follows,

$$\begin{aligned}\Delta x_n(t+2\tau) =&\Delta x_n(t+\tau)+\tau\left(V\left(\Delta x_{n+1}(t)\right)-V\left(\Delta x_n(t)\right)\right)+\lambda_1 p_0\left(-\Delta x_n(t+\tau)+\Delta x_n(t)\right)\\&+\lambda_2\left(1-p_0\right)\left(\Delta x_{n+1}(t+\tau)-\Delta x_{n+1}(t)-\Delta x_n(t+\tau)+\Delta x_n(t)\right),\end{aligned} \tag{8}$$

where $\tau = 1/\alpha$ represents the sensitivity coefficient of a driver to the difference between the optimal and the current velocities.

3. Linear stability analysis

We first study the stability of a uniform traffic flow. Uniform traffic flow is defined as a state in which all vehicles move with constant headway h and optimal velocity $V(h)$. Clearly, the steady-state solution of the model (8) is

$$x_{n,0}(t) = hn + V(h)t, \quad \text{with} \quad h = L/N, \tag{9}$$

where N is the total number of vehicles on the road, L is the length of the road, and $x_{n,0}(t)$ is the position of vehicle n in a steady state.

Let $y_n(t)$ be a small perturbation for the steady-state solution $x_{n,0}(t)$, then the perturbed solution is $x_n(t) = x_{n,0}(t)+y_n(t)$. Correspondingly, the headway can be expressed as $\Delta x_n(t) = h + \Delta y_n(t)$. Substituting these into Eq.(8), linearizing the equation, and neglecting the nonlinear terms, we obtain

$$\begin{aligned}\Delta y_n(t+2\tau) =&\Delta y_n(t+\tau)+\tau V'(h)\left(\Delta y_{n+1}(t)-\Delta y_n(t)\right)+\lambda_1 p_0\left(-\Delta y_n(t+\tau)+\Delta y_n(t)\right)\\&+\lambda_2\left(1-p_0\right)\left(\Delta y_{n+1}(t+\tau)-\Delta y_{n+1}(t)-\Delta y_n(t+\tau)+\Delta y_n(t)\right),\end{aligned} \tag{10}$$

where $V'(h) = \mathrm{d}V(\Delta x)/\mathrm{d}\Delta x$.

Expand Δy_n in the Fourier modes, i.e., $\Delta y_n(t) = A\exp(\mathrm{i}kn + zt)$. Then, Eq.(10) can be rewritten as

$$\begin{aligned}&\left(\mathrm{e}^{z\tau}-1\right)\left[\mathrm{e}^{z\tau}-\lambda\left(1-p_0\right)\left(\mathrm{e}^{\mathrm{i}k}-1\right)+\lambda p_0\right]\\&-\tau V'(h)\left(\mathrm{e}^{\mathrm{i}k}-1\right)=0.\end{aligned} \tag{11}$$

Solving Eq.(11) with respect to z, we find that the leading term of z is of the order of $\mathrm{i}k$. As $z \to 0$ when $\mathrm{i}k \to \infty$, we can express the long-wave solution of z as $z = z_1(\mathrm{i}k) + z_2(\mathrm{i}k)^2 + \ldots$. Inserting this into Eq.(11) and neglecting the second and higher order terms, we obtain two roots of z, as follows:

$$\begin{aligned}z_1 &= \frac{V'(h)}{1+\lambda_1 p_0},\\ z_2 &= \frac{V'(h)+2\lambda_2\left(1-p_0\right)z_1-\left(3+\lambda_1 p_0\right)\tau z_1^2}{2\left(1+\lambda_1 p_0\right)}.\end{aligned} \tag{12}$$

Clearly, the flow becomes unstable if $z_2 < 0$, and stable if $z_2 > 0$. Thus, the demarcation point between stable and unstable conditions (hereafter called the 'neutral stability point') is

$$\alpha = \frac{1}{\tau} = \frac{\left(3+\lambda_1 p_0\right)V'(h)}{\left(1+\lambda_1 p_0\right)^2+2\lambda_2\left(1-p_0\right)\left(1+\lambda_1 p_0\right)}. \tag{13}$$

If

$$\alpha < \frac{\left(3+\lambda_1 p_0\right)V'(h)}{\left(1+\lambda_1 p_0\right)^2+2\lambda_2\left(1-p_0\right)\left(1+\lambda_1 p_0\right)}, \tag{14}$$

then an unstable flow will evolve from a small perturbation in the uniform flow. We find that the neutral stability curve will drop with the increase of traffic interruption probability, which shows that the consideration of traffic interruption probability can improve the stability of traffic flow (shown in Fig.2).

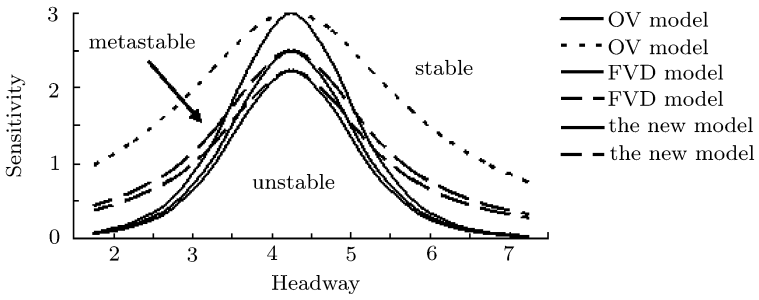


Fig.2. Phase diagram in the headway-sensitivity space. Each model has a pair of curves that have the same maximal sensitivity. The dotted curve is called 'coexisting curve' and the solid one 'neutral curve'. For each pair of curves, the space is divided into three regions by the two curves: the stable region above the coexisting curve, the metastable region between the neutral and coexisting curves, and the unstable region below the neutral curve. The parameters are set as follows: $\lambda_1 = 0.5,\ \lambda_2 = 0.1,\ p_0 = 0.2$.

For comparison purpose, the neutral curves given by the optimal velocity (OV) model and the full velocity difference (FVD) model are also depicted in Fig.2. It is easy to prove that $V'(h)$ reaches the maximal value of $0.5v_{\max}$ at the turning point $h = h_{\rm c}$, and thus the critical points $(h_{\rm c},\ \alpha_{\rm c})$ exist for these neutral stability curves. Figure 2 shows that with the same value of $h_{\rm c}$, the value of $\alpha_{\rm c}$ obtained from the proposed model is the lowest among those obtained from the other two models. This verifies that our model can improve the stability of traffic flow.

In order to further describe the effects of the traffic interruption probability on the stability of traffic flow, we next investigate the relationship between the critical value $\alpha_{\rm c}$ and the traffic interruption probability. The result is shown in Fig.3. It is found that $\alpha_{\rm c}$ decreases with the increase of the traffic interruption probability p_0. This implies that the stability of traffic flow can be improved if the following vehicle pays greater attention to the traffic interruption probability.

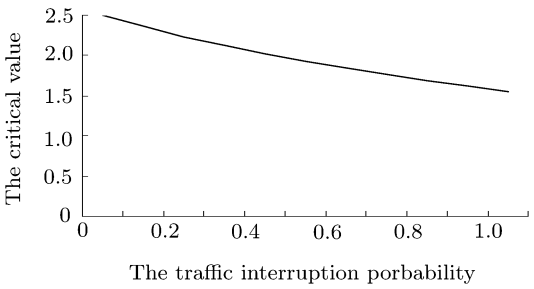


Fig.3. Relationship between the critical value $\alpha_{\rm c}$ and the traffic interruption probability p_0.

4. Nonlinear analysis

To further explore the effects of the traffic interruption probability on the stability of traffic flow, we conduct a nonlinear analysis of the slowly varying behaviour of long waves in the stable and unstable regions. We introduce the slow scales for space variable n and time variable t and define slow variables X and T as follows:

$$X = \varepsilon(n + bt) \ \text{ and } \ T = \varepsilon^3 t, \ \ 0 < \varepsilon \ll 1, \qquad (15)$$

where b is a constant to be determined later. Let

$$\Delta x_n(t) = h_{\rm c} + \varepsilon R(X, T), \qquad (16)$$

where $R(X,\ T)$ is a function to be determined. Substituting Eqs.(15) and (16) into Eq.(8), expanding ε by the Taylor series to the fifth order, we obtain the following nonlinear partial differential equation:

$$\begin{aligned} &\varepsilon^2 \left[Ab - V'(h_{\rm c})\right] \partial_X R + \varepsilon^3 A_3 \partial_X^2 R \\ &+ \varepsilon^4 \left(A\partial_T R + A_{41}\partial_X^3 R - A_{42}\partial_X R^3\right) \\ &+ \varepsilon^5((3b\tau + \lambda_1 p_0 b\tau - B)\,\partial_X \partial_T R \\ &+ A_{51}\partial_X^4 R - A_{52}\partial_X^2 R^3) = 0, \end{aligned} \qquad (17)$$

where

$$A = 1 + \lambda_1 p_0, \quad B = \lambda_2 \left(1 - p_0\right),$$

$$A_3 = \frac{3b^2\tau}{2} + \frac{\lambda_1 p_0 b^2 \tau}{2} - \frac{1}{2}V'(h_{\rm c}) - Bb,$$

$$A_{41} = \frac{7b^3\tau^2 + \lambda_1 p_0 b^3 \tau^2 - V'(h_{\rm c}) - B\left(3b + 3b^2\tau\right)}{6},$$

$$A_{42} = \frac{V'''(h_{\rm c})}{6},$$

$$A_{51} = \frac{5b^4\tau^3}{8} + \frac{\lambda_1 p_0 b^4 \tau^3}{24} - \frac{1}{24}V'(h_c) - B\left(\frac{4b + 6b^2\tau + 4b^3\tau^2}{24}\right),$$

$$A_{52} = \frac{V'''(h_c)}{12}, \quad V'(h_c) = \left.\frac{\mathrm{d}V(\Delta x)}{\mathrm{d}\Delta x}\right|_{\Delta x = h_c},$$

and

$$V'''(h_c) = \left.\frac{\mathrm{d}^3 V(\Delta x)}{\mathrm{d}\Delta x^3}\right|_{\Delta x = h_c}.$$

Setting $b = \dfrac{V'(h_c)}{A}$, then we can eliminate the terms of ε^2 from Eq.(17). We consider the neighbourhood of the critical point τ_c, such that

$$\tau/\tau_c = 1 + \varepsilon^2, \qquad ((18))$$

where $\tau_c = \dfrac{A^2 + 2AB}{CV'(h_c)}$, $C = 3 + \lambda_1 p_0$. Then, Eq.(17) can be rewritten as

$$\varepsilon^4\left(\partial_T R - m_1\partial_X^3 R + m_2\partial_X R^3\right) + \varepsilon^5\left(m_3\partial_X^2 R + m_4\partial_X^2 R^3 - m_5\partial_X^4 R\right) = 0, \qquad (19)$$

where

$$m_1 = -\frac{V'(h_c)}{6A^2C}\left\{(7 + \lambda_1 p_0)(A + 2B)^2 - AC^2 - B\left[3C^2 + 3(A + 2B)C\right]\right\},$$

$$m_2 = -\frac{V'''(h_c)}{6A},$$

$$m_3 = \frac{A + 2B}{2A^2}V'(h_c),$$

$$m_4 = \frac{V'''(h_c)}{12A},$$

and

$$m_5 = \frac{(15 + \lambda_1 p_0)(A + 2B)^3 - AC^3 - BC\left[4C + 6(1 + 2B)C + 4(A + 2B)^2\right]}{24A^2C^3}V'(h_c).$$

To derive the regularized equation, we make a transformation for Eq.(19), as follows:

$$\hat{T} = m_1 T, \quad R = \sqrt{\frac{m_1}{m_2}}\hat{R}. \qquad (20)$$

Then, Eq.(19) can be rewritten as the following regularized equation

$$\partial_{T'}R' = \partial_X^3 R' - \partial_X R'^3 - \varepsilon\left(\frac{27}{2}C_1\partial_X^2 R' + \frac{1}{2}C_2\partial_X^4 R' - \frac{1}{2}C_3\partial_X^2 R'^3\right), \qquad (21)$$

where $C_1 = \dfrac{m_3}{27m_1}$, $C_2 = \dfrac{2m_4}{m_1}$ and $C_3 = m_3$. If the perturbed term $O(\varepsilon)$ of Eq.(20) is ignored, Eq.(21) is just the modified KdV equation with kink solution as the desired solution,

$$R_0'(X, T') = \sqrt{c}\tanh\left(\sqrt{\frac{c}{2}}(X - cT')\right), \qquad (22)$$

where c is the propagation speed of the kink wave, which is determined by $O(\varepsilon)$. In order to determine c in Eq.(22), the following solvability condition should be satisfied,

$$(R_0', M[R_0']) \equiv \int_{-\infty}^{\infty}\mathrm{d}X R_0'(X, T')\, M\left[R_0'(X, T')\right] = 0, \qquad (23)$$

where

$$M\left[R_0'\right] = \sqrt{\frac{1}{m_1}}\left(m_3\partial_X^2 R' + \frac{m_1 m_4}{m_2}\partial_X^2 R'^3 - m_5\partial_X^4 R'\right).$$

Carrying out the integration, we can obtain the propagation speed,

$$c = \frac{135C_1}{2C_2 + 3C_3}. \qquad (24)$$

Thus, we derive the solution of the modified KdV equation, i.e.,

$$R(X, T) = \sqrt{\frac{m_1}{m_2}}\tanh\sqrt{\frac{c}{2}}(X - m_1 cT). \qquad (25)$$

If the optimal velocity takes the form Eq.(6), then $V'(h_c) = 1$ and $V'''(h_c) = -2$. The amplitude of the kink solution is given by

$$A^* = \left(\frac{m_1 c}{m_2}\left(\frac{\alpha_c}{\alpha} - 1\right)\right)^{1/2} \qquad (26)$$

with

$$\alpha_{\rm c} = \frac{CV'(h_{\rm c})}{A^2 + 2AB}. \tag{27}$$

The kink wave solution represents the coexisting phase, which consists of the freely moving phase with low density and the congested phase with high density. The headway of the freely moving phase is $\Delta x = h_{\rm c} + A^*$, and that of the congested phase is $\Delta x = h_{\rm c} - A^*$. Then, we can depict the coexisting curves in the parametrized space $(\Delta x,\ \alpha)$. Figure 2 shows the coexisting curves obtained by using the three models discussed in this paper. Each model has a pair of curves that have the same maximal sensitivity. The upper curve is the coexisting curve and the lower the neutral stability curve. For each pair of curves, the space is divided into three regions by the two curves: the stable region above the coexisting curve, the metastable region between the neutral and coexisting curves, and the unstable region below the neutral curve. It can be seen that both the neutral and the coexisting curves in our model decrease with the increase of the traffic interruption probability. Hence, the stability region is enlarged, and the metastable and unstable regions are reduced, when compared to other models. This verifies again that the consideration of traffic interruption probability can improve the stability of traffic flow.

5. Simulation

In this section, we use numerical results to explore the effects of the traffic interruption probability on the stability of traffic flow. The initial values of the model parameters in the simulation are given below:

$$\begin{cases} \Delta x_n(0) = \Delta x_n(1) = \Delta x_0, & n \neq 0.5N, n \neq 0.5N+1, \\ \Delta x_n(0) = \Delta x_n(1) = \Delta x_0 + 0.1, & n = 0.5N, \\ \Delta x_n(0) = \Delta x_n(1) = \Delta x_0 - 0.1, & n = 0.5N+1, \end{cases} \tag{28}$$

where $N(=200)$ is the number of vehicles and $\Delta x_0(=4.0)$ is the average headway. A periodic boundary condition is adopted in the simulation. Other parameters are

$$v_{\max} = 2.0, \quad \alpha = 2.0, \quad L = 800, \tag{29}$$

where L is the length of the studied highway. For simplicity, we in this paper assume that the traffic interruption probability be constant, i.e. $p_n = p_0 = 0.2$. Note that we only investigate the effects of the traffic interruption probability on the car-following behaviour and assume that there are no traffic interruptions on the circle road at all when we carry out the simulation.

Figure 4 shows the headway evolution after 10^4 time steps and the profile at $t = 10^4$. Figures 4(a)–4(d) are respectively the outputs of the OV model, the FVD model with $\lambda_2 = 0.1$, the FVD model with $\lambda_2 = 0.2$ and our new model with $\lambda_1 = 0.5,\ \lambda_2 = 0.2,\ p_0 = 0.2$. From this figure, we have the following results:

(i) In Figs.4(a)–4(c), stop-and-go traffic appears. It can be seen that the headway evolution and the profile are very similar to the solution of the mKdV equation. This is because the initial value condition lies in the unstable region if using the OV model and the FVD model to describe the small perturbations (24). When small perturbations are put into a uniform traffic flow, they are amplified with time, and consequently, the uniform traffic flow finally evolves into an inhomogeneous flow. The jam in Fig.4(a) is the most serious, followed by those in Fig.4(b) and Fig.4(c) since the relative velocity can improve the stability of traffic flow. In Fig.4(d), the perturbation finally disappears. This indicates that the introduction of traffic interruption probability can greatly improve the stability of traffic flow.

(ii) Figures 4(b) and 4(c) show that only considering relative velocity cannot completely eliminate perturbation although the relative velocity can improve the stability of traffic flow. Therefore, the traffic interruption probability should be considered in the car-following model for enhancing the stability of traffic flow.

(iii) The density waves in Figs.4(a)–4(d) always propagate backwards. This has been observed in reality and reported in the relevant research.

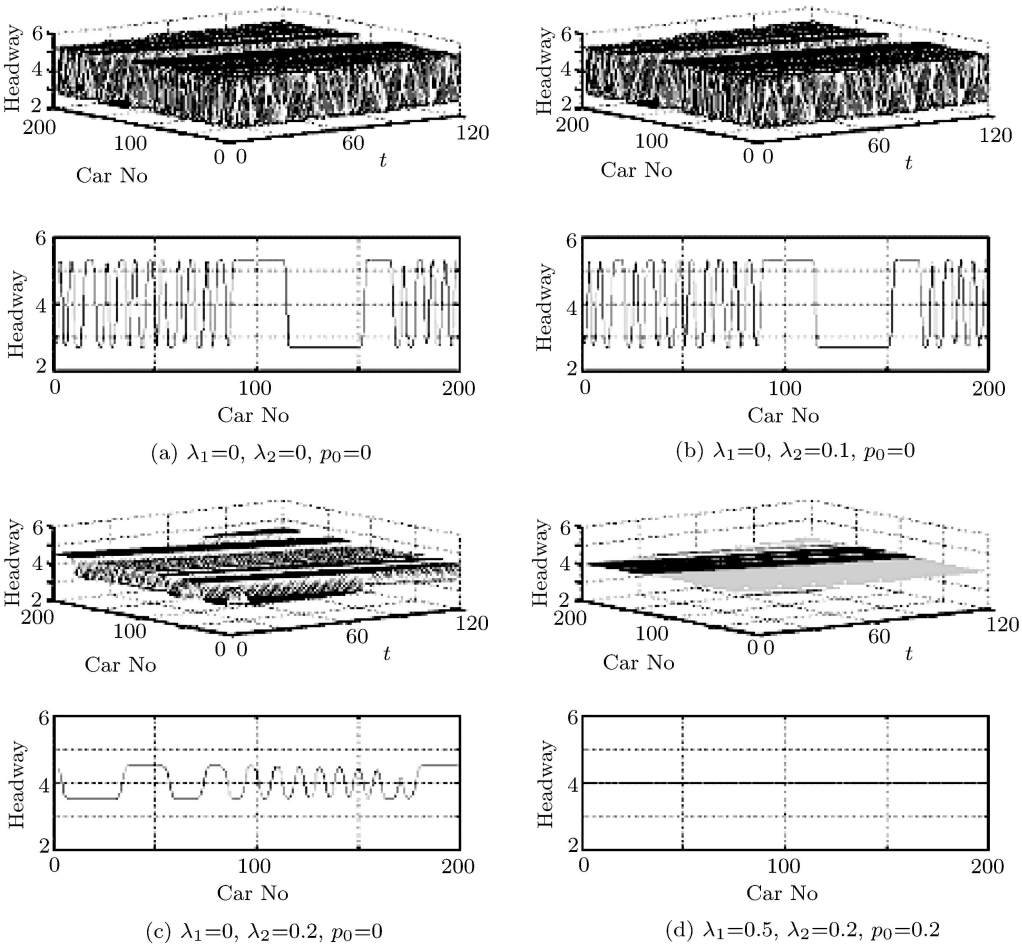


Fig.4. Headway evolution after 10^4 time steps and the profile at time step $t = 10^4$.

We next depict the velocity profiles at $t = 10^4$ under the small perturbation (28) (shown in Fig.5). Similar results to the points (i) and (ii) stated above can be concluded.

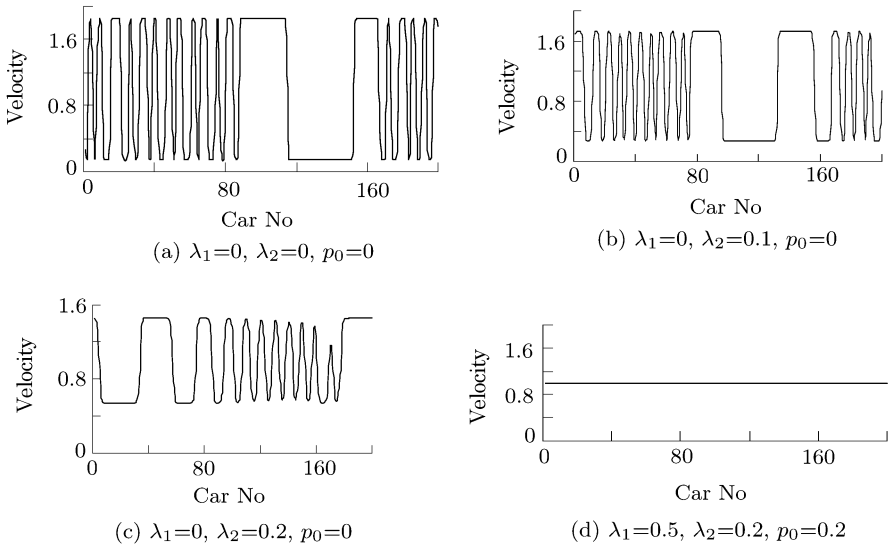


Fig.5. Velocity profile at time step $t = 10^4$.

In order to further prove that the consideration of the leading vehicle's traffic interruption probability can improve the stability of traffic flow, we now use Eq.(28) to analyse the effects of that the traffic interruption probability on the hysteresis loop (shown in Fig.6). From Fig.6, we find that the hysteresis loop of the new model is reduced to a point. This further verifies that the traffic flow stability is indeed improved by the consideration of traffic interruption probability.

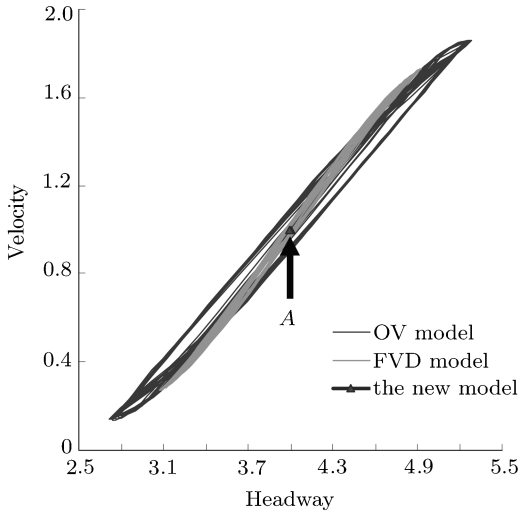


Fig.6. Hysteresis loops of the OV model, the FVD model and the new model. The parameters used are as follows: in the OV model, $\lambda_1 = \lambda_2 = p_0 = 0$; in the FVD model, $\lambda_1 = 0,\ \lambda_2 = 0.1,\ p_0 = 0$; in the new model, $\lambda_1 = 0.5,\ \lambda_2 = 0.2,\ p_0 = 0.2$.

6. Conclusions

In this paper, we have presented a new car-following model by taking into account the effects of the traffic interruption probability on the car-following behaviour of following vehicle. The stability of traffic flow has been analytically studied by using linear and nonlinear analyses. It has been shown that a critical point exists in the new model, and the neutral stability line and the coexisting curve are obtained. Obviously, a consideration of the traffic interruption probability can stabilize traffic flows. A modified KdV equation has been derived to describe traffic behaviour near the critical point. We demonstrate that the simulation results are consistent with the analytical results of the stability analyses. The numerical results about the space–time evolution of headway are accordant with the analytical results. It should be noted that in our model and simulation, traffic interruption does not happen really but is anticipated by the driver of the following vehicle when he or she makes a decision to accelerate or decelerate. Nevertheless, we find that such anxiety does indeed influence driving behaviour and stabilize traffic flow. In fact, there are many factors that have great effects on traffic interruption, for instance, the probability function of traffic interruption, the position and the last time of traffic interruption, the environment of road, the traffic density and others. The results reported in this paper rely on the assumed values of all parameters. It is of interest to calibrate these parameters by surveying data in order to optimize the performance of the model. In addition, the current work is limited in one-road system, however, extending it to a road network is valuable and challengeable.

References

[1] Chowdhury D, Santen L and Schadschneider A 2000 *Phys. Rep.* **329** 199
[2] Bando M, Hasebe K, Nakayama A, Shibata A and Sugiyama Y 1995 *Phys. Rev.* E **51** 1035
[3] Bando M, Hasebe K, Nakanishi K and Nakayama A 1998 *Phys. Rev.* E **58** 5429
[4] Davis L C 2002 *Phys. Rev.* E **66** 038101
[5] Lubashevsky I, Wagner P and Mahnke R 2003 *Eur. Phys. J.* B **32** 243
[6] Lubashevsky I, Wagner P and Mahnke R 2003 *Phys. Rev.* E **68** 056109
[7] Komatsu T S and Sasa S I 1995 *Phys. Rev.* E **52** 5574
[8] Helbing D and Tilch B 1998 *Phys. Rev.* E **58** 133
[9] Treiber M, Hennecke A and Helbing D 1999 *Phys. Rev.* E **59** 239
[10] Treiber M, Hennecke A and Helbing D 2000 *Phys. Rev.* E **62** 1805
[11] Jiang R, Wu Q S and Zhu Z J 2001 *Phys. Rev.* E **64** 017101
[12] Xue Y 2002 *Chin. Phys.* **11** 1128
[13] Xue Y 2003 *Acta Phys. Sin.* **52** 2750 (in Chinese)
[14] Li Z P and Liu Y C 2006 *Chin. Phys.* **15** 1570
[15] Nagatani T 1999 *Phys Rev.* E **60** 6395

[16] Lenz H, Wagner C K and Sollacher R 1999 *Eur. Phys. J.* B **7** 331

[17] Hasebe K, Nakayama A and Sugiyama Y 2003 *Phys. Rev.* E **68** 026102

[18] Hasebe K, Nakayama A and Sugiyama Y 2004 *Phys. Rev.* E **69** 017103

[19] Ge H X, Dai S Q, Dong L Y and Xue Y 2004 *Phys. Rev.* E **70** 066134

[20] Zhao X M and Gao Z Y 2005 *Eur. Phys. J.* B **47** 145

[21] Wang T, Gao Z Y and Zhao X M 2006 *Acta Phys. Sin.* **55** 634 (in Chinese)

[22] Han X L, Jiang C Y, Ge H X and Dai S Q 2007 *Acta Phys. Sin.* **56** 4383 (in Chinese)

[23] Wong S C, Leung B S Y, Loo B P Y, Hung W T and Lo H K 2004 *Accident Analysis and Prevention* **36** 281

[24] Wong S C, Sze N N and Li Y C 2007 *Accident Analysis and Prevention* **39** 1107

[25] Sze N N and Wong S C 2007 *Accident Analysis and Prevention* **39** 1267

[26] Telesca L and Lovallo M 2008 *Physica* A **387** 3299

[27] Baykal-Gürsoy M, Xiao W and Ozbay K 2009 *Eur. J. Oper. Res.* **195** 127